Supplementary information

Sensitive Detection and Prostate Cancer Cellular Evaluation of Sarcosine via a Fluorescence Turn-On Assay Using an N-CQDs/Ag^+ Nanosensor

Xinyu Shen[1#], Suli He[2#], Lezhong Qi[1], Xiayong Jing[1], Xinqiang Gan[1], Xingjun He[1*]

[1]Department of Urology, Affiliated Hospital of Yangzhou University, No. 368 Hanjiang Middle Road, Yangzhou, Jiangsu, China

[2]Department of Obstetrics and Gynecology, Affiliated Hospital of Yangzhou University, No. 45 Taizhou Road, Yangzhou, Jiangsu, China

[#]These authors contributed equally to this work.

[*]Corresponding author: Xingjun He

E-mail: xingjunhe1982@163.com

Materials and Reagents

Sarcosine oxidase (SOx, from Bacillus sp., ≥95% purity, activity ≥20 U/mg), sarcosine (≥98%), silver nitrate ($AgNO_3$, ≥99.8%), and all other salts and chemicals were of analytical reagent grade and purchased from Sigma-Aldrich (St. Louis, MO, USA) or Aladdin Biochemical Technology Co., Ltd. (Shanghai, China). Phosphate-buffered saline (PBS, 10 mM, pH 7.4) was prepared using sodium phosphate dibasic and sodium phosphate monobasic. All aqueous solutions were prepared using ultrapure water (resistivity ≥18.2 MΩ·cm) from a Millipore Milli-Q system.

The human prostate cell lines used in this study were obtained from the Cell Bank of the Chinese Academy of Sciences (Shanghai, China). These included the androgen-independent prostate cancer cell line PC-3, the androgen-sensitive prostate cancer cell line LNCaP, and the benign prostatic hyperplasia epithelial cell line BPH-1, which served as a non-malignant control.

Instrument

Fluorescence emission and excitation spectra were recorded on a Hitachi F-7100 fluorescence spectrophotometer (Tokyo, Japan) equipped with a 150 W xenon lamp. For all measurements, the excitation and emission slit widths were set at 5.0 nm. Ultraviolet-visible (UV-vis) absorption spectra were acquired using a Shimadzu UV-2700 spectrophotometer (Kyoto, Japan). The morphology and size of the nanomaterials were characterized by transmission electron microscopy (TEM) on a JEOL JEM-2100 microscope (Tokyo, Japan) operating at an acceleration voltage of 200 kV. For TEM sample preparation, a droplet of the diluted nanoparticle suspension was placed onto a carbon-coated copper grid and air-dried at room temperature. X-ray photoelectron spectroscopy (XPS) analysis was performed on a Thermo Scientific K-Alpha+ spectrometer (Waltham, MA, USA). All cell culture procedures were conducted in the incubator (Thermo Fisher Scientific, USA) maintained at 37 °C with a humidified atmosphere of 5% CO_2.

Synthesis of N-CQDs

N-doped carbon quantum dots (N-CQDs) were synthesized via a facile one-pot hydrothermal method. Briefly, 2.0 g of thoroughly washed and vacuum-dried castor seeds were ground into fine powder, dispersed in 30 mL deionized water, and sonicated at room temperature for 30 min to form a uniform suspension. The dispersion was transferred into a 50 mL Teflon-lined stainless-steel autoclave, sealed, and heated in an electric oven at 180 °C for 10 h. After natural cooling to ambient temperature, the resulting brownish solution was centrifuged at 8000 rpm for 15 min, filtered through a 0.22 μm hydrophilic PVDF membrane, and dialyzed (MWCO: 1000 Da) against deionized water for 48 h (water renewed every 12 h) to remove impurities and small-molecule byproducts. The purified N-CQDs aqueous solution was stored in a sealed container at 4 °C for subsequent use.

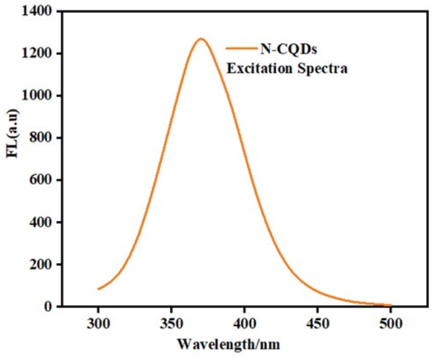

Figure S1. Excitation spectra of the N-CQDs.

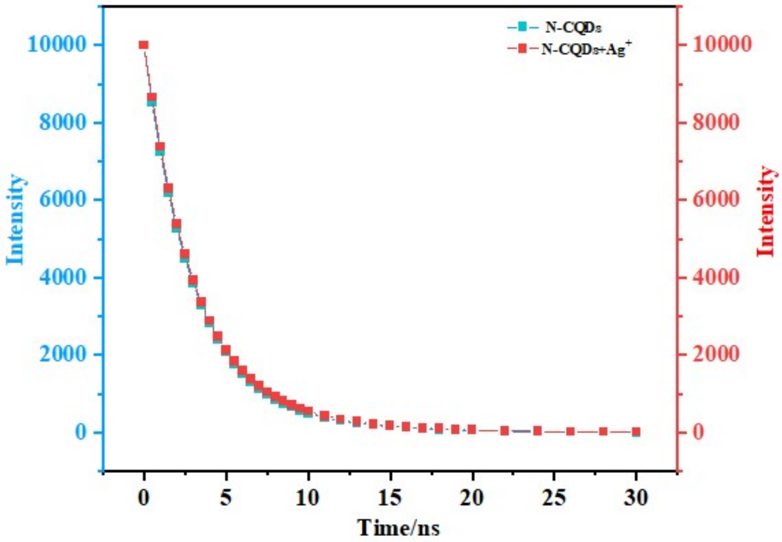

Figure S2. Fluorescence decay curves of N-CQDs in the absence (green squares) and presence (red circles) of 100 μM Ag^+. Excitation wavelength: 380 nm; emission monitored at 450 nm. The nearly identical decay profiles indicate that the fluorescence quenching by Ag^+ follows a static quenching mechanism, consistent with the formation of a non-fluorescent ground-state N-CQDs/Ag^+ complex.

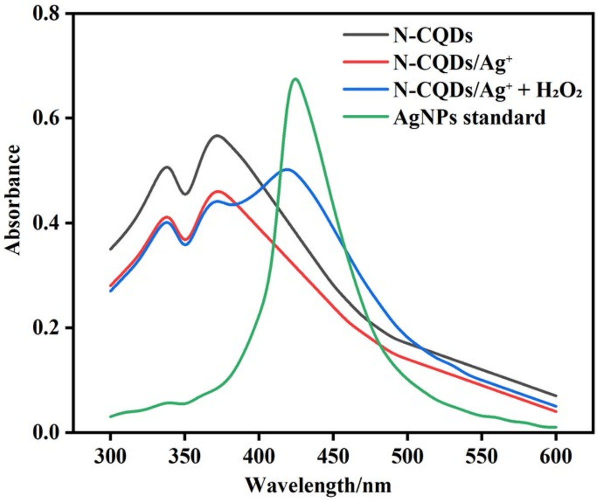

Figure S3. UV-Vis absorption spectra confirming the H_2O_2-mediated reduction of Ag^+ to Ag^0. Spectra of N-CQDs alone (black), N-CQDs/Ag^+ (red), and N-CQDs/Ag^+ after treatment with H_2O_2 (blue), and spectrum of the Ag NP standard (green).

Table S1. Spike recovery of sarcosine in fetal bovine serum (FBS) at different concentrations

Spiked Sarcosine (μM)	Measured Sarcosine (μM)	Recovery (%)	RSD (%, n=3)
10.0	10.25	98.3	4.1
20.0	19.60	95.9	2.6
40.0	39.45	97.6	2.4

Table S2. Comparison of the proposed method with existing analytical methods for sarcosine detection

Method	Material/ Platform	LOD (μM)	Linear Range (μM)	Detection Time	Advantages	Limitations	Ref
This work	**N-CQDs/Ag$^+$**	**2.1**	**10-60**	**30 min**	**Turn-on, selective, cell-compatible**	**Moderate LOD**	**—**
LC-MS/MS	—	0.00005-0.004	0.003-40	Hours	Ultra-high sensitivity, accurate	Expensive, complex, not POC	[S1]
Fluorescence (turn-on)	Co-doped CQDs	1.54	0–10	Not specified	Turn-on, sensitive	Narrow linear range	[S2]
Ratiometric fluorescence	MOF nanozyme	0.03998	Not specified	Not specified	Ultra-sensitive	Complex preparation	[S3]
Colorimetric	Various nanozymes	0.008-500	0.1-100	Minutes	Simple, low-cost	Lower sensitivity	[S4]
Electrochemical	CoNiWBO/rGO	0.04	0.1-50	Fast	Portable, rapid, non-enzymatic	Stability issues	[S5]
Electrochemical	Various electrodes	Down to nM	Variable	Fast	Portable, rapid	Stability issues	[S6]
Colorimetric (MIP)	Zn/Ce-ZIF@MIP	Not specified	Not specified	Minutes	High specificity, molecular imprinting	Complex preparation	[S7]

References

[S1] Jiang Y, Cheng X, Wang C, et al. Quantitative determination of sarcosine and related compounds in urinary samples by liquid chromatography with tandem mass spectrometry. Analytical chemistry, 2010, 82(21): 9022-9027.

[S2] Zeyadi M, Chaudhari K G, Patil P O, et al. Development of a highly sensitive fluorescent probe using Delonix regia (Gulmohar) tree pod shell for precise sarcosine detection in human urine samples: advancing prostate cancer diagnosis. Journal of Biomolecular Structure and Dynamics, 2025, 43(10): 4928-4941.

[S3] Hou J, Wang J, Han J, et al. An intelligent ratiometric fluorescent assay based on MOF nanozyme-mediated tandem catalysis that guided by contrary logic circuit for highly sensitive sarcosine detection and smartphone-based portable sensing application. Biosensors and Bioelectronics, 2024, 249: 116035.

[S4] Venugopal Iyer V, Rajendran R, Selvaraj S. Colorimetric and electrochemical sensors for the detection of sarcosine, a potential biomarker for prostate cancer: a review. Current Analytical Chemistry, 2024, 20(1): 2-13.

[S5] Wasim M, Shaheen S, Fatima B, et al. Non-enzymatic electrochemical detection of sarcosine in serum of prostate cancer patients by CoNiWBO/rGO nanocomposite. Scientific Reports, 2024, 14(1): 24240.

[S6] Pundir C S, Deswal R, Kumar P. Quantitative analysis of sarcosine with special emphasis on biosensors: a review. Biomarkers, 2019, 24(5): 415-422.

[S7] Liu P, Liu Y, Gai Z, et al. Highly specific colorimetric detection of sarcosine using surface molecular imprinted Zn/Ce-ZIF. Journal of Colloid and Interface Science, 2025, 681: 239-249.